



Aalborg Universitet

AALBORG UNIVERSITY  
DENMARK

## Uncertainty quantification of the dynamics of a wave energy converter

Moura Paredes, Guilherme; Eskilsson, Claes; Kofoed, Jens Peter

*Published in:*  
VIII International Conference on Computational Methods in Marine Engineering

*Publication date:*  
2019

*Document Version*  
Publisher's PDF, also known as Version of record

[Link to publication from Aalborg University](#)

*Citation for published version (APA):*  
Moura Paredes, G., Eskilsson, C., & Kofoed, J. P. (2019). Uncertainty quantification of the dynamics of a wave energy converter. In R. Bensow, & J. Ringsberg (Eds.), *VIII International Conference on Computational Methods in Marine Engineering: MARINE 2019* (pp. 157-168). International Center for Numerical Methods in Engineering.

### General rights

Copyright and moral rights for the publications made accessible in the public portal are retained by the authors and/or other copyright owners and it is a condition of accessing publications that users recognise and abide by the legal requirements associated with these rights.

- Users may download and print one copy of any publication from the public portal for the purpose of private study or research.
- You may not further distribute the material or use it for any profit-making activity or commercial gain
- You may freely distribute the URL identifying the publication in the public portal -

### Take down policy

If you believe that this document breaches copyright please contact us at [vbn@aub.aau.dk](mailto:vbn@aub.aau.dk) providing details, and we will remove access to the work immediately and investigate your claim.

# UNCERTAINTY QUANTIFICATION OF THE DYNAMICS OF A WAVE ENERGY CONVERTER

Guilherme Moura Paredes<sup>\*1</sup>, Claes Eskilsson<sup>\*2</sup> Jens Peter Kofoed<sup>\*3</sup>

<sup>\*</sup>Aalborg University  
Department of Civil Engineering  
Thomas Manns vej 23, DK-9220 Aalborg Ø, Denmark  
e-mail: <sup>1</sup>gmp@civil.aau.dk, <sup>2</sup>cge@civil.aau.dk, <sup>3</sup>jpk@civil.aau.dk

**Key words:** Uncertainty Quantification, Sensitivity Analysis, General Polynomial Chaos, Wave Energy Converter, Power Take-off; Numerical Simulation

**Abstract.** Since time-domain simulations of wave energy converters are computationally expensive, how can we analyse their dynamics and test wide ranges of design variables, without simplifying the physics involved? One possible solution is the use of General Polynomial Chaos (gPC). GPC provides computationally efficient surrogate models for partial differential equation based models, which are particularly useful for sensitivity analysis and uncertainty quantification. We demonstrate the application of gPC to study the dynamics of a wave energy converter in an operational sea-state, when there is uncertainty in the values of the stiffness and damping coefficient of the power take-off.

## 1 INTRODUCTION

In wave energy, time-domain simulations are unappealing because of the complexity of non-linear effects and the long computational time required. Even the most simple simulations resorting to linear potential flow theory can be time consuming. To complicate this situation, in uncertainty quantification traditional Monte-Carlo (MC) based methods require thousands upon thousands of time-domain simulations to obtain statistical distributions of the quantities of interest. However, this situation can be overcome using General Polynomial Chaos (gPC), and we will demonstrate its application to study the operation of a wave energy converter.

Our case study, described in Section 3, will be a simple two-body heaving point absorber, with a quadratic power take-off, and a three-leg catenary mooring system. In this example, the stiffness and the damping coefficient of the power take-off (PTO) will be the variables subjected to uncertainty, and we will study how the mooring tension, the body motions and the absorbed power is influenced by the uncertainty (Section 4).

General Polynomial Chaos, briefly explained in Section 2.1, provides a polynomial expansion surrogate model for partial differential equation (PDE)-based numerical models with random inputs [1]. Its application to study random processes and uncertainty quantification has several advantages over traditional MC-based methods. Unlike MC methods, gPC does not require

thousands of simulations to obtain stable values for the mean and variance. Using gPC, depending on the specific method, chosen the mean and variance can be obtained with only tens of simulations. Another advantage is that the statistical distributions of the quantities of interest can be obtained by running very large samples of the random inputs through the gPC surrogate model, which can be orders of magnitude faster to run than the PDE-based numerical model.

Polynomial Chaos was first described in 1938 by Norbert Wiener [2], for expansions using only Gauss's distribution. In 2002 it was expanded by Xiu and Karniadakis [3] to expansions using other statistical distributions, for improved convergence in cases where the quantities of interest do not have a gaussian distribution. Since then it has been used in a wide range of applications. One expected application, which drives many of the publications regarding gPC is uncertainty quantification in CFD [4, 5, 6]. Other applications are the study of the dynamics of train wagons [7], electronic circuits [8], particle physics [9], among many more. In ocean and coastal engineering, gPC has been applied in the analys wave scattering from an ice floe [10], propagation of water waves over uneven bottoms [11], to study a heaving buoy in irregular waves [12], just to name a few. More interestingly, in 2018 Lim *et al* [13] applied gPC to determine the extreme loads on the power take-off of a heaving wave energy converter.

## 2 THEORY

### 2.1 General polynomial chaos

Consider a process with both deterministic and uncertain inputs:

$$\mathbf{f} = \mathbf{f}(\mathbf{x}, \mathbf{Z}) \quad (1)$$

where  $\mathbf{f}$  is a general function,  $\mathbf{x}$  is the vector of deterministic inputs and  $\mathbf{Z}$  is the vector of uncertain inputs (or random variables) with dimension  $d$ . The gPC surrogate model of  $\mathbf{f}$  is given by a polynomial expansion of the form [1]:

$$\mathbf{f}_{\text{gPC}}(\mathbf{x}, \mathbf{Z}) = \sum_{|\mathbf{k}|=0}^{\infty} \hat{\mathbf{f}}_{\mathbf{k}}(\mathbf{x}) \Psi_{\mathbf{k}}(\mathbf{Z}) = \sum_{|\mathbf{k}|=0}^{\infty} \hat{\mathbf{f}}_{\mathbf{k}}(\mathbf{x}) \psi_{k_1}(Z_1) \psi_{k_2}(Z_2) \dots \psi_{k_d}(Z_d) \quad (2)$$

where  $\hat{\mathbf{f}}_{\mathbf{k}}$  are the polynomial coefficients,  $\mathbf{k} = (k_1, k_2, \dots, k_d) \in \mathbb{N}_0$  is a multi-index,  $|\mathbf{k}| = k_1 + k_2 + \dots + k_d$ , and  $\psi_{k_i}(Z_i)$  is the polynomial basis function of the variable  $Z_i$ , of degree  $k_i$ . Because the expansion in Eq. (2) is an infinite series, it needs to be truncated to a chosen polynomial degree  $p$  for practical use, becoming:

$$\mathbf{f}_{\text{gPC}}(\mathbf{x}, \mathbf{Z}) \approx \sum_{|\mathbf{k}|=0}^p \hat{\mathbf{f}}_{\mathbf{k}}(\mathbf{x}) \Psi_{\mathbf{k}}(\mathbf{Z}) = \sum_{|\mathbf{k}|=0}^p \hat{\mathbf{f}}_{\mathbf{k}}(\mathbf{x}) \psi_{k_1}(Z_1) \psi_{k_2}(Z_2) \dots \psi_{k_d}(Z_d) \quad (3)$$

The degree  $p$  of the polynomial expansion must be selected depending on the needs of each particular case study. It can be chosen by trial and error, until a sufficiently accurate representation of the model is achieved, or by examining the value of the polynomial coefficients which, for smooth solutions, decay quickly with increasing  $p$ . For the selection of the polynomial family

$\psi_{k_i}(Z_i)$ , the Weiner-Askey scheme provides the polynomials that converge optimally to solution of some of the most common statistical distributions [3].

There are two ways to apply gPC to a PDE-based model: the Stochastic Galerkin method and the Stochastic collocation method. The Stochastic Galerkin method is classified as intrusive because it needs the underlying equations of the numerical model to be reformulated. This can be complicated, and sometimes impossible, either because of mathematical complexity, or simply because there is no access to the code of the numerical model. The Stochastic collocation method is much simpler to apply because it does not depend on the numerical model, it does not need access to the code, nor re-casting of the differential equations. All that is needed is to run simulations on a selected number of collocation nodes  $\mathbf{z}_j$ , and post-process the results.

In our analysis we will be studying a process with only two random variables,  $d = 2$ . In this case, the gPC coefficients can be efficiently computed using the projection method. This is the inner product of the process  $\mathbf{f}(\mathbf{x}, \mathbf{Z})$  and the polynomial basis functions  $\Psi_{\mathbf{k}}(\mathbf{Z})$ , with respect to the probability density function of the random variables,  $\rho(\mathbf{Z})$  Eq. (4):

$$\langle \hat{f}_{\mathbf{k}}(\mathbf{x}), \Psi_{\mathbf{k}}(z) \rangle = \frac{\int f(\mathbf{x}, \mathbf{z}) \Psi_{\mathbf{k}}(\mathbf{z}) \rho(\mathbf{z}) d\mathbf{z}}{\int \Psi_{\mathbf{k}}^2(\mathbf{z}) \rho(\mathbf{z}) d\mathbf{z}} \quad (4)$$

The integration of Eq. (4) is done using quadrature rules, such as Gauss quadrature, which provide the points  $\mathbf{z}^{(j)}$  where the model is to be evaluated, and the quadrature weights,  $\mathbf{w}^{(j)}$ .

The interaction between the different univariate polynomials in the tensor product can be controlled through the  $q$ -norm. A  $q$ -norm of 1 allows the tensor product of any set of univariate polynomials to reach the maximum selected polynomial order; decreasing the  $q$ -norm, until the minimum value of zero, decreases the maximum polynomial order allowed for products of univariate polynomials, reducing the total number of polynomial terms.

For smooth solutions, gPC shows exponential convergence. It is because of this, and because the mean and variance are encoded in the gPC coefficients, that it is possible to obtain stable values of the mean and variance using fewer simulations than in MC-based methods. Depending on the normalization used for the polynomials  $\psi_{k_i}(Z_i)$ , the mean is  $\hat{\mathbf{f}}_0$ , while the variance is the sum of the squares of  $\{\hat{f}_k(\mathbf{x})\}_{k=1}^p$  (or scaled values of these).

For the computation of the gPC model we used UQLab's version 1.0.0, Polynomial Chaos Expansions Module [14].

## 2.2 Hydrodynamic, cable, and PTO models

The dynamics of the wave energy converter were modelled in WEC-Sim [15, 16], a time-domain solver for wave energy converters based on Cummins's equation [17]. The PTO selected for the wave energy converter was an hydraulic one, represented by the following model [18]:

$$f_{\text{pto}}(u, v) = ku + c_{\text{hyd}}v|v| \quad (5)$$

where  $f_{\text{pto}}$  is the force applied by the PTO,  $k$  is the linear stiffness of the PTO,  $u$  and  $v$  are, respectively, the relative displacement and velocity between the bodies driving the PTO, and  $c_{\text{hyd}}$  is the hydraulic damping coefficient of the PTO.

The mooring system was modelled in MooDy [19]. MooDy is an *hp*-adaptive discontinuous Galerkin (DG) numerical model for mooring cables, based on the equation of motion of cables with neither bending nor torsional stiffness. WEC-Sim and MooDy were coupled for the simultaneous simulation of dynamics of the wave energy converter and of the mooring systems; this coupling has been validated and demonstrated in [20].

### 2.3 Model equations with random inputs

Because of the uncertainty in the inputs, the model equations describing the dynamics of a moored wave energy converter become stochastic equations, with some variables becoming dependent on the uncertain inputs,  $\mathbf{Z}$ . In our analysis, the uncertain inputs are the stiffness,  $k$ , and damping coefficient,  $c_{\text{hyd}}$  of the PTO:

$$\mathbf{Z} = (k, d) \quad (6)$$

As presented in [21], Cummins's equation is now written as:

$$\mathbf{M} + \mathbf{A}_\infty \ddot{\mathbf{x}}(t, \mathbf{Z}) + \int_{-\infty}^t \mathbf{K}(t - \tau) \dot{\mathbf{x}}(t, \mathbf{Z}) d\tau + \mathbf{C}\mathbf{x}(t, \mathbf{Z}) = \mathbf{f}_{\text{ext}}(t) + \mathbf{f}_{\text{moor}}(t, \mathbf{Z}) + \mathbf{f}_{\text{pto}}(t, \mathbf{Z}) \quad (7)$$

where  $\mathbf{M}$  is the generalised mass matrix,  $\mathbf{A}_\infty$  is the matrix of added mass at infinity,  $\mathbf{K}$  is the radiation impulse response function,  $\mathbf{C}$  is the stiffness matrix,  $\ddot{\mathbf{x}}$ ,  $\dot{\mathbf{x}}$ , and  $\mathbf{x}$  are, respectively, the acceleration, velocity, and position vectors of the floating bodies,  $\mathbf{f}_{\text{moor}}(t, \mathbf{Z})$  is the mooring force,  $\mathbf{f}_{\text{pto}}(t, \mathbf{Z})$  is the PTO force,  $\mathbf{f}_{\text{ext}}(t)$  is the vector of remaining external forces non-dependent on the uncertain input  $\mathbf{Z}$ , and  $t$  is time. In its turn, the equation of motion of mooring cables becomes [21]:

$$m_l(s) \frac{\partial^2 \mathbf{r}(s, t, \mathbf{Z})}{\partial t^2} = \left( \frac{T(\epsilon(s, t, \mathbf{Z}))}{1 + \epsilon(s, t, \mathbf{Z})} \frac{\partial \mathbf{r}(s, t, \mathbf{Z})}{\partial s} \right) + \frac{\partial}{\partial s} + \mathbf{f}_e(s, t, \mathbf{Z}), \quad (8a)$$

$$\epsilon(s, t, \mathbf{Z}) = \left| \frac{\partial \mathbf{r}(s, t, \mathbf{Z})}{\partial s} \right| - 1 \quad (8b)$$

where  $m_l$  is the mass per unit length of the cable,  $\mathbf{r}$  is the position vector of a point  $s$  of the cable, where  $s$  is measured along the unstretched length of the cable,  $T$  is the tension magnitude,  $\epsilon$  is the extension, and  $\mathbf{f}_e$  is the vector of external forces acting on the cable. Finally, the equation of the hydraulic PTO, Eq. (5) becomes

$$f_{\text{pto}}(u, v, \mathbf{Z}) = f_{\text{pto}}(u, v, k, c_{\text{hyd}}) = ku + c_{\text{hyd}}v|v| \quad (9)$$

where  $k$  and  $c_{\text{hyd}}$  are now random variables.

### 3 CASE STUDY

Our case study is based on the moored RM3 device tutorial distributed with WEC-Sim, Figure 1. The RM3 device is an axisymmetric two-body heaving point-absorber, using the relative motion between the two bodies to generate energy. The mooring system has been simplified from its original set-up, and here it is composed only of simple chains without floaters, Figure 1 and Table 1.

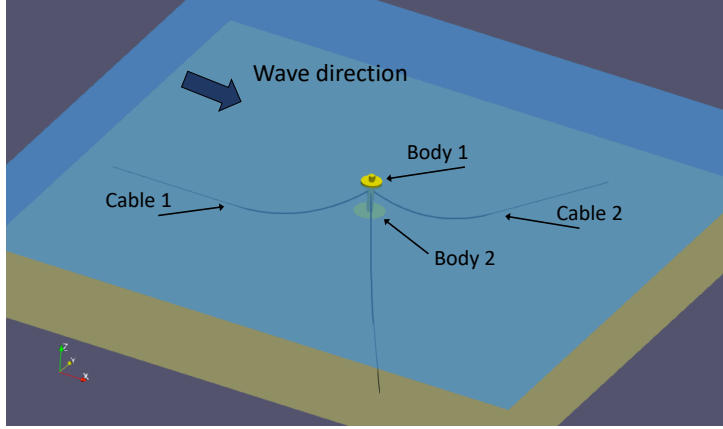


Figure 1: The RM3 case device and set-up.

Table 1: Parameters of the mooring cables.

| Quantity                                   | Value                  |
|--|------------------------|
| Diameter ( $D_c$ )                         | 0.144 m                |
| Density ( $\gamma_c$ )                     | 7736 kg/m <sup>3</sup> |
| Stiffness ( $EA$ )                         | 583.376 MN             |
| Normal drag coefficient ( $C_{dn}$ )       | 1.6                    |
| Tangential drag coefficient ( $C_{dt}$ )   | 0.5                    |
| Normal added mass coefficient ( $C_{an}$ ) | 1                      |
| Cable length                               | 280 m                  |

We attributed to the PTO's stiffness,  $k$ , and damping coefficient,  $c_{hyd}$ , uniform distributions with the parameters presented in Table 2. The uniform distribution, attributing equal probability to all values, can both represent uncertainty and be used for sensitivity analysis. In WEC-Sim, the device was modelled using the one-hour irregular wave time-series umpqua46229\_6\_2008 provided with the tutorial, and a time-step of 0.01 s. The mooring systems was simulated in MooDy [19], using, for each cable, 10 elements of order 5, with an adaptive time-step to ensure the Courant-Friedrichs-Lewy condition did not exceed 0.9.

To create the gPC model we used the quadrature method, testing increasing polynomial

Table 2: Probabilistic distributions for the parameters of the PTO.

| Parameter        | Deterministic value                         | Distribution | Lower bound                                 | Upper bound                                 |
|------------------|---|--------------|---|---|
| $k$              | $1.0 \times 10^4 \text{ N/m}$               | Uniform      | $7.0 \times 10^3 \text{ N/m}$               | $1.3 \times 10^4 \text{ N/m}$               |
| $c_{\text{hyd}}$ | $1.20 \times 10^6 \text{ N s}^2/\text{m}^2$ | Uniform      | $4.80 \times 10^5 \text{ N s}^2/\text{m}^2$ | $1.92 \times 10^6 \text{ N s}^2/\text{m}^2$ |

orders until we achieved convergence of the probability distribution functions (PDF). The PDFs were created, for each time-step and for each output variable, by first running 3000 random sample pairs of  $k$  and  $c_{\text{hyd}}$  through the gPC model; then, using kernel density estimation, the probability density functions were smoothed. The final polynomial order selected for the gPC model was 9, requiring 100 simulations in total to determine the gPC coefficients.

#### 4 RESULTS

In Figure 2 we show the time-series of the rigid body motions, power absorbed, and tension in the mooring cables of the RM3 device, for the simulation using the deterministic values of  $k$  and  $c_{\text{hyd}}$ . In Figure 3 we show the evolution of the PDFs of the same variables at  $t = 3000 \text{ s}$ , as we increase the polynomial order of the gPC model. We can see that, for a polynomial order of 9, all the PDFs have converged. However, some PDFs converged much earlier: the PDF of the heave motion of body 2 had already converged for order 1, presenting an almost uniform distribution of its values.

In Figure 4 we show the 95% confidence intervals for the different output variables. We plot only a small portion of the whole time-series, centred around  $t = 3000 \text{ s}$ , because otherwise it was not possible to visualise the confidence intervals. For comparison, this figure shows also simulation results using the deterministic values of  $k$  and  $c_{\text{hyd}}$ . Although  $k$  has a variation of 30% around its deterministic value, and  $c_{\text{hyd}}$  has a variation of 60%, the confidence intervals are quite narrow. The only exception is the confidence interval for the absorbed power, which shows a wide confidence interval at highest power peaks. This means that, to some extent, the power extracted by the device can be increased, without significantly changing motions of the floating WEC or the loads on the mooring cables. One possible explanation for narrow confidence intervals is the small value of the PTO's damping coefficient, associated with small velocities induced by the waves. For the RM3 device equipped with a linear PTO, values of linear damping coefficient up to around  $2.5 \times 10^6 \text{ N s/m}$  correspond to very under-damped motions [22]. In our case, the PTO depends on the square of the velocity and the maximum value is  $1.92 \times 10^6 \text{ N s/m}$ , which, when motions are small, place it in the under-damped region. In this range of operation, even the relatively large variations of  $k$  and  $c_{\text{hyd}}$  generate only relatively small perturbations of the dynamics of the device.

Other reason for the narrow confidence intervals is the possibility that the WEC might not be operating in its most favourable sea-state (or the relatively small amplitude of the waves in the tested sea-state) which might not induce large enough motions. Finally, because WEC-Sim does not account for second order drift forces, the loads in the mooring cables are somewhat smaller than they would be if second order loads were accounted for, which might also help to explain the narrow confidence intervals.

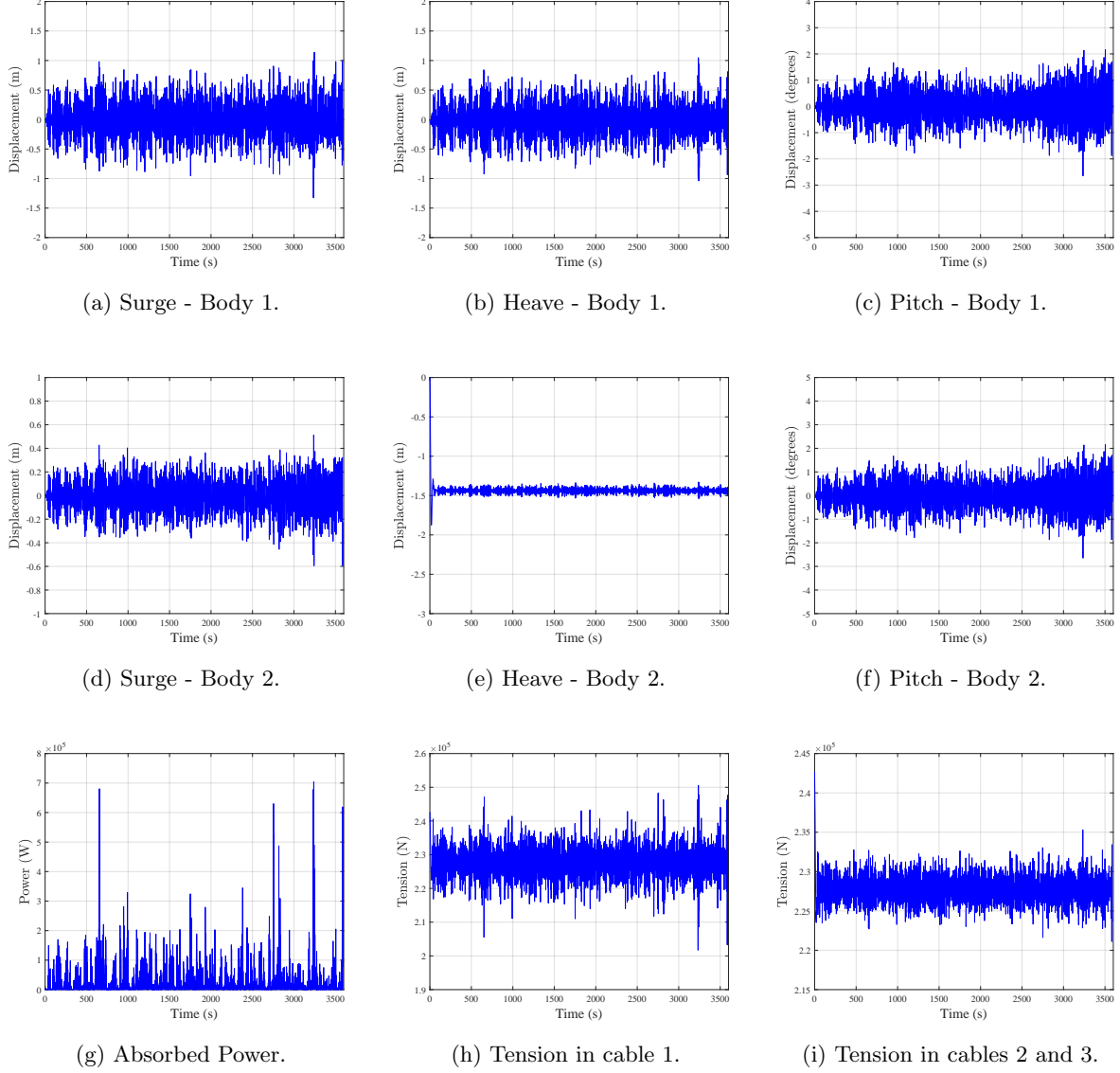


Figure 2: Time-series of displacement in surge, heave and pitch, absorbed power, and tension in the mooring cables for the RM3 device.

In Figure 4 we did not plot mean values of the simulation results, because they are almost the same as the simulation results using the deterministic values of  $k$  and  $c_{\text{hyd}}$ . Since the deterministic values of  $k$  and  $c_{\text{hyd}}$  are also their mean, this shows that the mean of the outputs is similar to the outputs computed using the mean inputs. In other other words, the simulations are almost linear. This is probably due to the device having only small motions in the tested sea-state, that do not generate large velocities in the power take-off, nor fast motions of the mooring cables, which are the major non-linear components.



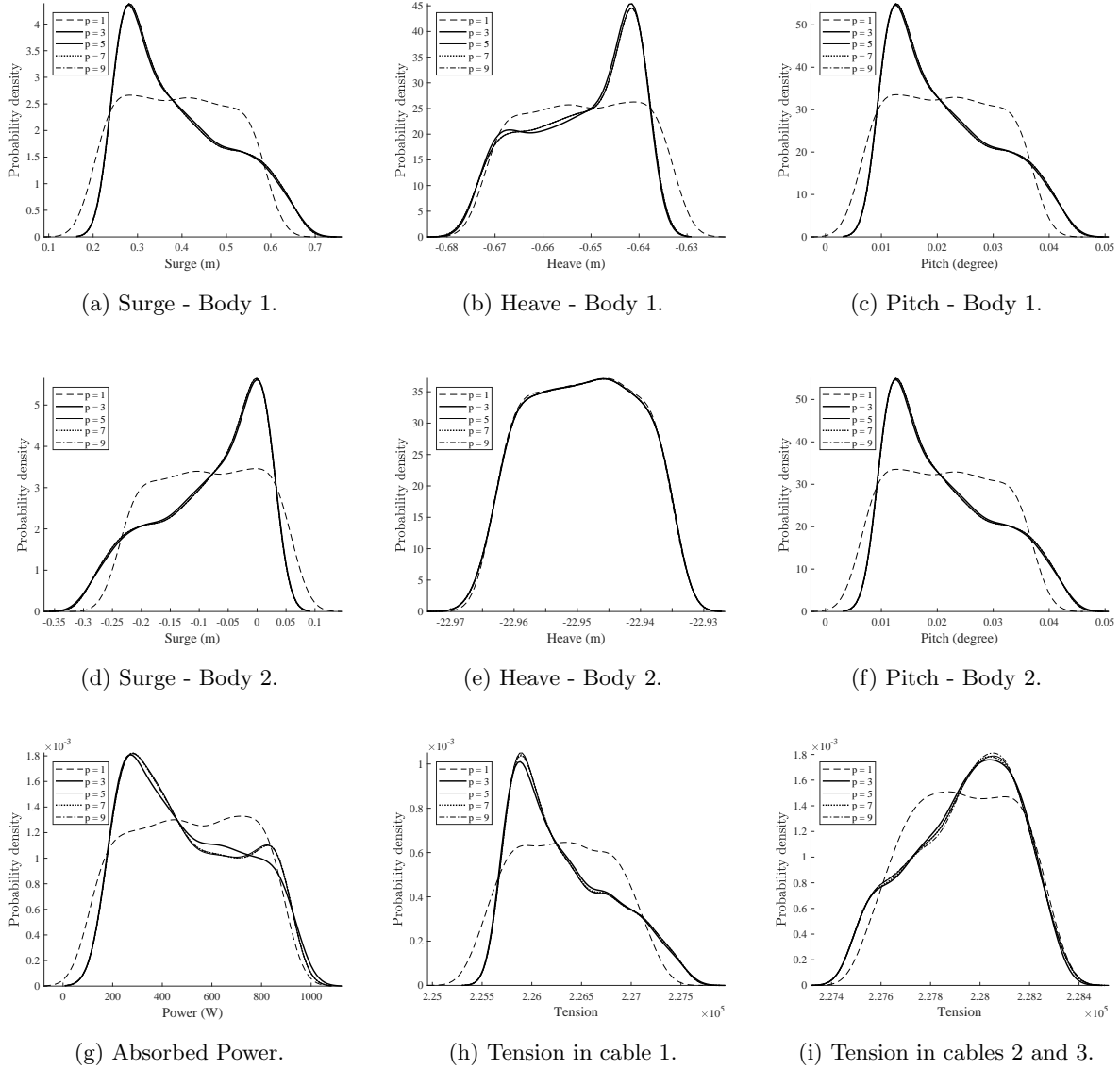
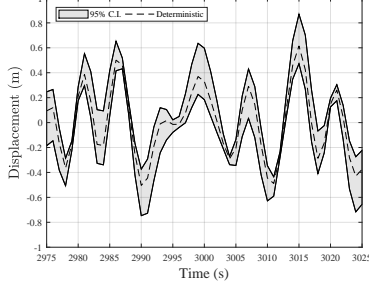
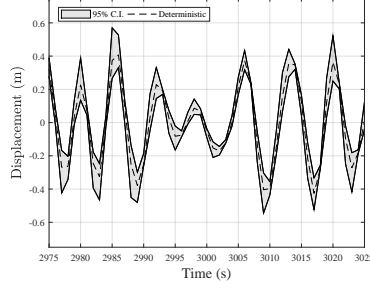


Figure 3: Convergence of the probability density function of displacement, power, and tension in the cables at time instant  $t = 3000$  s.

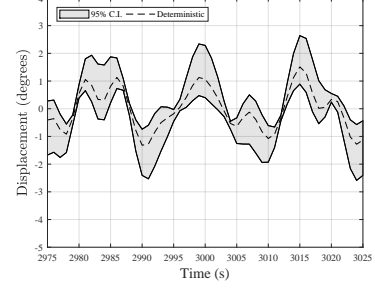
Looking at the confidence interval for heave of body 2, Figure 4e, we can see that both the mean and the deterministic value lie almost in the center of the confidence interval. This, and its almost uniform PDF at  $t = 3000$  s, Figure 3e, point to heave in body 2 being a linear function of  $k$  and  $c_{hyd}$ .



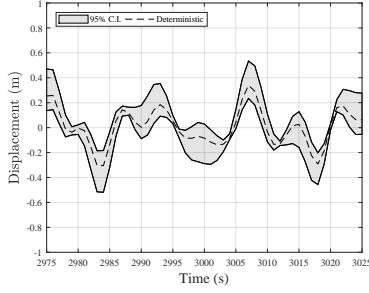
(a) Surge - Body 1.



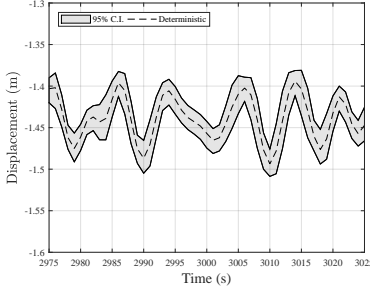
(b) Heave - Body 1.



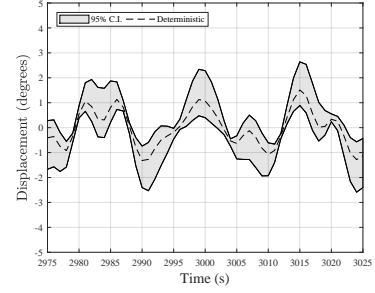
(c) Pitch - Body 1.



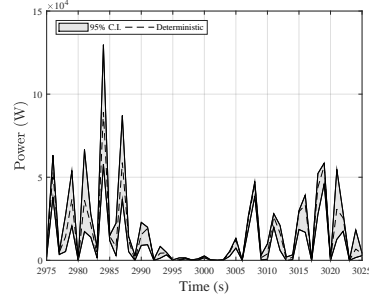
(d) Surge - Body 2.



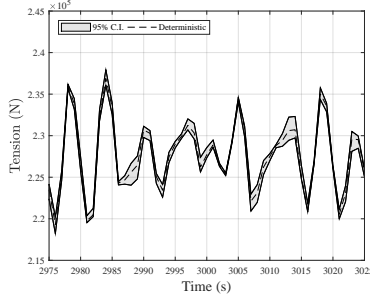
(e) Heave - Body 2.



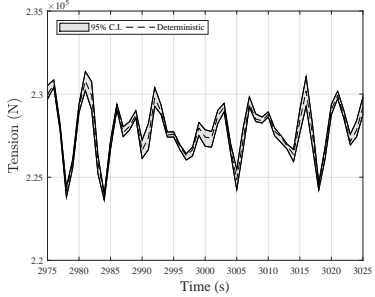
(f) Pitch - Body 2.



(g) Absorbed Power.



(h) Tension in cable 1.



(i) Tension in cables 2 and 3.

Figure 4: 95% confidence interval and deterministic value of of displacement, power, and tension in the cables of the RM3 device.

## 5 CONCLUSIONS

We presented a case study of the dynamics of moored a wave energy converter, when the stiffness and damping coefficient of its quadratic hydraulic power take-off are uncertain. The wave energy converter analysed was the RM3 two-body heaving point absorber developed by NREL and Sandia. To propagate the uncertainty in the parameters of the PTO to the dynamics of the converter, we used general Polynomial Chaos, in its Stochastic Collocation formulation. Our general Polynomial Chaos model used 9<sup>th</sup> order polynomials to represent surge, heave, pitch, mooring cable tension, and extracted power as a function of PTO stiffness and damping coefficient.

By applying general Polynomial Chaos, we were able to obtain the equivalent of 3000 time-domain simulations of the RM3 device with as many different values of PTO stiffness and damping coefficients, when in fact we ran only 100 simulations in the numerical model. General Polynomial Chaos allows a fast and efficient analysis of non-linear processes and time-consuming simulations. For the particular case of wave energy, general Polynomial Chaos is useful even for devices with a linear PTO, as, for a large number of test cases, or when modelling non-linear mooring systems, the simulations will take considerable time.

The results we obtained showed that, for the case analysed, even though there was a significant uncertainty attributed to the stiffness and damping coefficient of the power take-off (30% and 60%, respectively), the motions and tensions in the mooring cables did not show a wide variability. This might be due to the damping coefficient of the power take-off being too low, even at the maximum value of the uncertainty interval, to have a significant influence on the dynamics of the wave energy converter. It can also be due to the wave amplitude and periods of the sea-state not inducing large enough motions on the device.

Because what we presented was a relatively simple application case of general Polynomial Chaos, future work on this topic should focus on testing a wider range of PTO stiffness and damping coefficient values, different distributions, a larger variety of sea-states, as well as longer sea-states.

## REFERENCES

- [1] Dongbin Xiu. *Numerical Methods for Stochastic Computations - A Spectral Method Approach*. Princeton University Press, Princeton, New Jersey, 2010.
- [2] Norbert Wiener. The Homogeneous Chaos. *American Journal of Mathematics*, 60(4):897, 1938.
- [3] Dongbin Xiu and George Em Karniadakis. The Wiener-Askey Polynomial Chaos for Stochastic Differential Equations. *SIAM Journal on Scientific Computing*, 24(2):619–644, jan 2002.
- [4] O. P. Le Maître and Omar M. Knio. *Spectral Methods for Uncertainty Quantification*. Scientific Computation. Springer Netherlands, Dordrecht, 2010.
- [5] Vincent Couaillier and Eric Savin. Generalized Polynomial Chaos for Non-intrusive Uncertainty Quantification in Computational Fluid Dynamics. In *Uncertainty Management for Robust Industrial Design in Aeronautics*, pages 123–141. 2018.

- [6] Chris Lacor and Éric Savin. *General Introduction to Polynomial Chaos and Collocation Methods*, pages 109–122. Springer International Publishing, 2019.
- [7] D. Bigoni, H. True, and A.P. Engsig-Karup. Sensitivity analysis of the critical speed in railway vehicle dynamics. *Vehicle System Dynamics*, 52:272–286, 2014.
- [8] P. Manfredi, D. Vande Ginste, D. De Zutter, and F. G. Canavero. Generalized decoupled polynomial chaos for nonlinear circuits with many random parameters. *IEEE Microwave and Wireless Components Letters*, 25(8):505–507, Aug 2015.
- [9] M. M. R. Williams. Polynomial chaos functions and neutron diffusion. *Nuclear Science and Engineering*, 155(1):109–118, 2007.
- [10] J. E. M. Mosig, F. Montiel, and V. A. Squire. Water wave scattering from a mass loading ice floe of random length using generalised polynomial chaos. *Ocean Modelling*, 70:239, 2017.
- [11] Daniele Bigoni, Allan P. Engsig-Karup, and Claes Eskilsson. Efficient uncertainty quantification of a fully nonlinear and dispersive water wave model with random inputs. *Journal of Engineering Mathematics*, 101:87–113, 2016.
- [12] Edwin Kreuzer and Eugen Solowjow. Polynomial Chaos and the Heave Motion of a Cylinder in Random Seas. In *Proceedings in Applied Mathematics and Mechanics*, volume 15, pages 559–560. Springer, 2015.
- [13] HyeonGuk Lim, Lance Manuel, and Ying Min Low. On Efficient Long-Term Extreme Response Estimation for a Moored Floating Structure. In *Volume 3: Structures, Safety, and Reliability*, page V003T02A043. ASME, 2018.
- [14] S. Marelli and B. Sudret. Uqlab user manual - polynomial chaos expansions. Technical report, Chair of Risk, Safety & Uncertainty Quantification, ETH Zurich, Zurich, 2018.
- [15] National Renewable Energy Laboratory and Sandia Corporation. WEC-Sim (Wave Energy Converter SIMulator) WEC-Sim documentation, 2015.
- [16] Yi-Hsiang Yu, Michael Lawson, Kelley Ruehl, and Carlos Michelen. Development and demonstration of the WEC-Sim wave energy converter simulation tool. In *Proceedings of the 2nd Marine Energy Technology Symposium METS2014*, page 8, Seattle, WA, USA, 2014. Marine Energy Technology Symposium.
- [17] W. E. Cummins. The impulse response function and ship motions. Technical report, David Taylor Model Basin, Washington D. C., 1962.
- [18] Helen Louise Bailey. *Effect of a nonlinear power take off on a wave energy converter*. PhD Thesis, The University of Edinburgh, 2011.
- [19] Johannes Palm, Claes Eskilsson, and Lars Bergdahl. An hp-adaptive discontinuous Galerkin method for modelling snap loads in mooring cables. *Ocean Engineering*, 144:266–276, 2017.

- [20] Guilherme Moura Paredes, Claes Eskilsson, Johannes Palm, Jens Peter Kofoed, and Lars Bergdahl. Coupled BEM/hp-FEM Modelling of Moored Floaters. In *Proceedings of the 1st Vietnam Symposium on Advances in Offshore Engineering. VSOE 2018*, pages 504–510. Hanoi, 2018.
- [21] Guilherme Moura Paredes, Claes Eskilsson, and Allan P.; Engsig-Karup. Uncertainty Quantification in Mooring Cable Dynamics Using Polynomial Chaos Expansions. *Submitted for possible publication*, 2019.
- [22] Vincent S Neary, Michael Lawson, Mirko Previsic, Andrea Copping, Kathleen C Hallett, Alison Labonte, Jeff Rieks, and Dianne Murray. Methodology for Design and Economic Analysis of Marine Energy Conversion (Mec) Technologies. Technical report, Sandia National Laboratories, 2014.